

Reconstruction of Undersampled Atomic Force Microscopy Images

Interpolation versus Basis Pursuit

Jensen, Tobias Lindstrøm; Arildsen, Thomas; Østergaard, Jan; Larsen, Torben

Published in:

The 9th International Conference on Signal Image Technology and Internet Based Systems

DOI (link to publication from Publisher):

[10.1109/SITIS.2013.32](https://doi.org/10.1109/SITIS.2013.32)

Publication date:

2013

Document Version

Accepted author manuscript, peer reviewed version

[Link to publication from Aalborg University](#)

Citation for published version (APA):

Jensen, T. L., Arildsen, T., Østergaard, J., & Larsen, T. (2013). Reconstruction of Undersampled Atomic Force Microscopy Images: Interpolation versus Basis Pursuit. In *The 9th International Conference on Signal Image Technology and Internet Based Systems* (pp. 130 - 135). IEEE Computer Society Press.
<https://doi.org/10.1109/SITIS.2013.32>

General rights

Copyright and moral rights for the publications made accessible in the public portal are retained by the authors and/or other copyright owners and it is a condition of accessing publications that users recognise and abide by the legal requirements associated with these rights.

- Users may download and print one copy of any publication from the public portal for the purpose of private study or research.
- You may not further distribute the material or use it for any profit-making activity or commercial gain
- You may freely distribute the URL identifying the publication in the public portal -

Take down policy

If you believe that this document breaches copyright please contact us at vbn@aub.aau.dk providing details, and we will remove access to the work immediately and investigate your claim.

RECONSTRUCTION OF UNDERSAMPLED ATOMIC FORCE MICROSCOPY IMAGES: INTERPOLATION VERSUS BASIS PURSUIT

T. L. Jensen, T. Arildsen, J. Østergaard, T. Larsen

Signal and Information Processing,
Dept. of Electronic Systems, Aalborg University, Denmark
{tlj,tha,jo,tl}@es.aau.dk

ABSTRACT

Atomic force microscopy (AFM) is one of the most advanced tools for high-resolution imaging and manipulation of nanoscale matter. Unfortunately, standard AFM imaging requires a timescale on the order of seconds to minutes to acquire an image which makes it complicated to observe dynamic processes. Moreover, it is often required to take several images before a relevant observation region is identified. In this paper we show how to significantly reduce the image acquisition time by undersampling. The reconstruction of an undersampled AFM image can be viewed as an inpainting, interpolating problem, or a special case of compressed sensing. We argue that the preferred approach depends upon the type of image. Of the methods proposed for AFM, images containing high frequencies should be reconstructed using basis pursuit from data collected in a spiral pattern. Images without too much high frequency content should be reconstructed using interpolation.

Index Terms—Undersampling, imaging, sampling patterns

I. INTRODUCTION

AFM images are traditionally obtained using conventional Shannon-Nyquist sampling theory, where each line is uniformly sampled by a raster scan which leads to slow acquisition [1], [2], [3]. Conventional AFM acquisition time is of the order of seconds to minutes [4]. Traditional approaches for improving imaging speed for AFM are twofold [5], see also the discussion in [2], [4]: 1) Improving imaging hardware, e.g., reducing cantilever size and actuator design. 2) Improving the controller and the controller algorithm. The solutions proposed are all well motivated and engineered but all use the tools of the engineering disciplines dominating AFM. Recently, we have seen solutions originating in imaging and signal processing [6], [7], [8], including compressed sensing [9], [4], which give new possibilities to AFM imaging. Notice that these image processing improvements can essentially be applied along with any

improvement of hardware and controller. In that sense, the hardware/controller/image processing techniques are not competing but can offer complementary improvements to AFM imaging.

There are three main arguments for reducing the image acquisition time in atomic force microscopy [1], [5], [4]: 1) reduction of the tedious waiting time and increased productivity; 2) possibility to study dynamic processes, often denoted video-rate AFM; 3) reducing the applied force to avoid damage and modification of the scanned matter. An extension to the first argument is to use fast AFM for previewing — to help the user locate a region of interest. Following an acceptable preview, the user can then obtain a high-quality image for various applications, publishing etc.

A strategy to decrease the acquisition time is to reduce the number of measurements e.g. by simply skipping a number of complete horizontal lines when scanning the object [8], or using a square pattern [9], [4]. Another interesting pattern is the spiral sampling pattern which has the advantage that it can be used with most modern AFM hardware [10] but has yet not been used for undersampled images.

AFM is a versatile tool and is used in many different types of engineering and sciences [3]. This means that the AFM images can have many different characteristics. We explore these differences to propose image-class-dependent reconstruction methods. Measurement imperfections such as tilt and non-linearities etc. are not included, see e.g. [3], and instead the focus is on various computationally efficient reconstruction methods and their performance on different types of images. The ideas presented in the present paper apply to all imaging systems that obtain measurements directly in the image domain. One such group of systems is scanning probe microscopes in general, but in this paper we focus on the AFM application.

The rest of the paper is organized as follows. In Sec. II we present the model for undersampled data acquisition and in Sec. III we discuss different methods for reconstruction and the selection of a suitable dictionary. Sec. IV discuss different type of images and V presents simulations and comparison. Sec. VI discusses the results and provide conclusions of the paper.

The work is supported by The Danish Council for Strategic Research under grant number 09-067056, The Danish Council for Independent Research under grant number 1335-00278 and the Danish Center for Scientific Computing

II. MEASUREMENT SYSTEM

In this paper we consider one-channel (grey-scale) images of dimension $m \times n$, represented by $X \in \mathbb{R}^{m \times n}$. For the mathematical notation that follows, it is useful to represent the image X by the vector $x = \text{vec}(X) \in \mathbb{R}^{N \times 1}$ stacked column-wise from X with $mn = N$. The measurements can then be seen as a matrix-vector multiplication of x by a selection matrix $\Phi \in \{0, 1\}^{M \times N}$, $M \leq N$, where each row of Φ contains exactly one element with a one. One possible realization is

$$\Phi = \begin{bmatrix} 1 & 0 & 0 & \cdots & 0 & 0 \\ 0 & 0 & 1 & \cdots & 0 & 0 \\ \vdots & 0 & \ddots & \ddots & \vdots & \vdots \\ 0 & 0 & 0 & \cdots & 1 & 0 \end{bmatrix}. \quad (1)$$

The function $h(x) = \Phi x$ is sometimes referred to as a masking function. The system then obtains the measurements

$$y = \Phi x + e \quad (2)$$

where $y \in \mathbb{R}^{M \times 1}$ are the observed measurements and $e = y - \Phi x \in \mathbb{R}^{M \times 1}$ accounts for the remaining error (measurement noise, model inaccuracies etc.). Reconstructing $\hat{x} \simeq x$ from y can be seen as an inpainting problem, a problem that is closely connected to inverse problems and compressed sensing [11], or interpolation. Since we assume $M \leq N$, we have the sampling ratio

$$\kappa = \frac{M}{N} \in [0, 1]. \quad (3)$$

A traditional compressed sensing approach to undersampling often uses random sampling [12]. One way of obtaining random samples is to measure at random points. Due to the physical mechanism of the AFM system, this does not offer a significantly lower acquisition time, even though the number of measurements is significantly lower [4]. If the AFM probe tip is instead moved along a continuous trajectory, sampling the image along the way, the acquisition time can be reduced by exactly the fraction κ of the measurements taken [4].

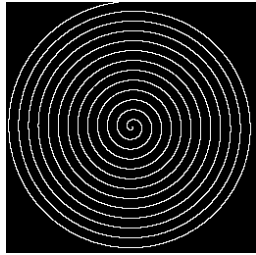


Fig. 1: Example spiral pattern; $\kappa = 0.1$, 256×256 grid.

A continuous trajectory already proposed for AFM is the spiral pattern [10]. However, in [10] the distance between two lines of the raster scan is equal to the pitch of the

spiral pattern in this investigation and the image is hence not undersampled. This however exemplifies that it is possible to implement the spiral sampling pattern in AFM imaging systems. Similar ideas of non-raster patterns without undersampling has previously been exploited using Lissajous patterns [13], [14]. A more direct approach is to only select a few lines in the traditional raster scan and then use standard interpolation or inpainting techniques [8]. To illustrate, Fig. 1 shows a spiral sampling pattern.

III. RECONSTRUCTION

Many methods have been proposed for obtaining $\hat{x} \simeq x$ from the model described by (2), see e.g. [15], [11]. One well-known and -proven method is the basis pursuit denoising model

$$\begin{aligned} &\text{minimize} \quad \|z\|_1 \\ &\text{subject to} \quad \|Az - y\|_2 \leq \delta \end{aligned} \quad (4)$$

where $A = \Phi\Psi \in \mathbb{R}^{M \times K}$ is a combination of the measurement system Φ and a dictionary $\Psi \in \mathbb{R}^{N \times K}$, δ accounts for noise in the observations. By reconstructing with (4) using $A = \Phi\Psi$, we should take care when constructing/selecting the dictionary Ψ . A wavelet dictionary may be used since these are known to be able to sparsely represent many natural images. However, the limited support of wavelets and high undersampling can generate zero columns in A and hence poor reconstruction. Therefore, the (fully dense) discrete cosine transform (DCT) is used as dictionary (as in [9], [4]) to be able to handle any sampling ratios.

Basis pursuit reconstruction methods enjoy some of the strongest known guarantees for reconstruction albeit algorithms for solving (4) are more computationally demanding than other methods, see [16]. However, the time frame for acquisition in AFM actually suits the time frame of reconstruction via the model (4) on a standard computer. This makes reconstruction via (4) practically feasible as demonstrated in the simulations section.

In terms of more classic inpainting and interpolation methods, it seems inconclusive which methods are preferred [8], but (bi)cubic interpolation seems to perform reasonably. We compare the basis pursuit approach to a classical interpolation approach in Sec. V-A.

IV. IMAGE CHARACTERISTICS

Since AFM is a versatile tool, many different types of images could be acquired by an AFM system. However, the accuracy of different reconstruction method also depends on the image. It is well-known that interpolation methods cannot reconstruct aliased high-frequency information. On the other hand, basis-pursuit can reconstruct all frequencies, including high frequencies. This motivates the two classes:

- Class I: Images without strong high-frequency components.*
- Class II: Images with strong high-frequency components.*

To quantify if an image is class I or class II, let $\tilde{X} = \mathcal{D}(X)$ be the DCT of the image X and

$$\Omega_\tau = \left\{ (k_1, k_2) \mid \sqrt{k_1^2 + k_2^2} \leq \frac{m+n}{2}\tau, \right. \\ \left. k_1 = 1, \dots, m, k_2 = 1, \dots, n \right\}. \quad (5)$$

The energy ratio comparing the energy in the low frequencies of the DCT to the total energy is then

$$\rho_\tau = \frac{\sum_{(k_1, k_2) \in \Omega_\tau} |\tilde{X}[k_1, k_2]|^2}{\sum_{k_1=1}^m \sum_{k_2=1}^n |\tilde{X}[k_1, k_2]|^2} \in [0, 1]. \quad (6)$$

The value ρ_τ is a measure of frequency content and can be used as a metric that assists in distinguishing the two classes. Specifically, a high ρ_τ is an indicator of class I and a low ρ_τ is an indicator of class II. Since the meaning of high/low frequency content should be measured relative to the sampling ratio we select $\tau = \kappa$. This selection gives no aliasing in the reconstruction when using an ideal sinc reconstruction filter if the signal is uniformly sampled and $\rho_\kappa = 1$ (any rate above κ is oversampling). Class I is then all images $\mathcal{I}(\kappa)$ with $\rho_\kappa > 0.25$ and class II is then $\mathcal{J}(\kappa)$ with $\rho_\kappa \leq 0.25$. Examples of class I images are images of e.g. cells and class II images are images with fine details and a periodic tendency across the image. To exemplify this, 32 test images are obtained from an AFM image library, which is available online¹. Fig. 2 shows two of these test images and their frequency content (DCT).

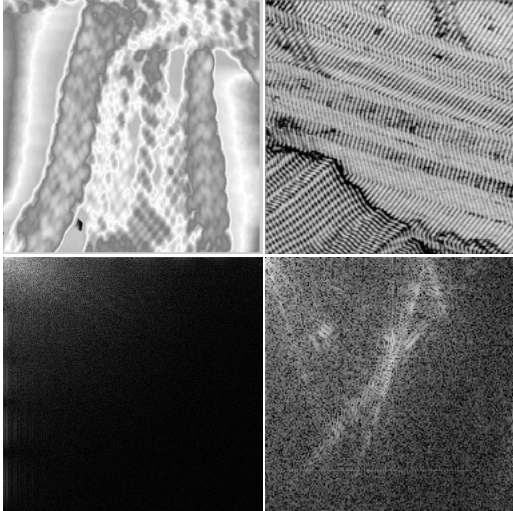


Fig. 2: Left: Thiophene molecules ($\rho_{0.1} = 0.888$, class I). Right: Alkane $C_{36}H_{72}$ ($\rho_{0.1} = 0.249$, class II). Top: image domain. Bottom: corresponding frequency content.

¹We obtain all images that are not rotated or with text inclusion from <http://nano.tm.agilent.com/index.php/image-library>. In total 32 AFM images used in various applications in life and materials science.

V. SIMULATION SETUP

The problem described by (4) is solved using SPGL1 [17]². The test images are of high quality but from noisy measurements so we select δ such that we have a peak-signal-to-noise-ratio (PSNR) of the observed data y of 40 dB. The images used in these simulations are not sparse but compressible (see e.g. [12]), so perfect reconstruction is not possible unless $\kappa \simeq 1$. The reconstruction time to approximately solve (4) or performing a (bi)cubic interpolation is denoted by t .³

Another possible scan trajectory is a square pattern [9], [4]. In almost all of our experiments, either subline sampling with interpolation (SIP) or spiral pattern sampling with basis pursuit reconstruction (SBP) performed better than a square sampling pattern with basis pursuit reconstruction (SQBP). Where SQBP was observed to give a higher PSNR, it was only a marginal improvement ($\simeq 0.1$ dB) and the square patterns usually contained more distinct reconstruction artifacts. The reconstruction choice therefore seems to be between SBP or SIP, as further analyzed in Sec. V-A.

V-A. Comparison

In Fig. 3 we examine a $(m, n) = (454, 454)$ AFM image of endothelial cells representing a clear case of image class I ($\rho_{0.1} = 0.961$). In Fig. 3 the spiral scan sampling provides a modest PSNR and clear reconstruction artifacts. The interpolation-based approach both gives a significantly higher PSNR and less reconstruction artifacts. The reconstructions are not perfect but seem acceptable for preview. We note that for measuring PSNR with the spiral pattern, we have an error floor because the corners are not reconstructed well. Since conventional AFM acquisition time is of the order of seconds to minutes [4], a reconstruction time on the order 1–10 s seems acceptable.

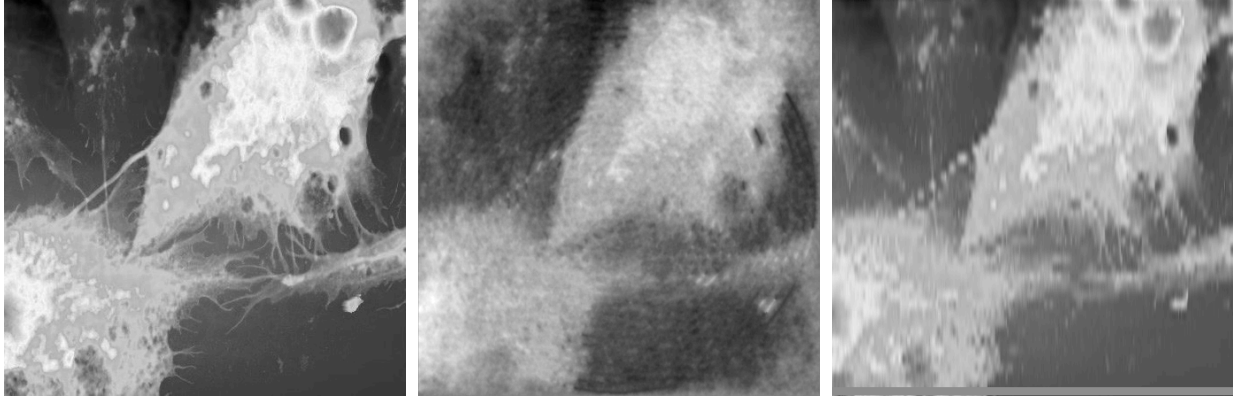
In Fig. 4 we examine a $(m, n) = (256, 254)$ AFM image of an atomic lattice representing a clear case of image class II ($\rho_{0.1} = 0.001$). In Fig. 4, the spiral scan sampling provides a modest PSNR and some reconstruction artifacts. The interpolation-based approach gives a low PSNR and clear reconstruction artifacts and aliasing-effects. Notice that SBP reconstruction time is only 1.8 s.

Table I gives average PSNR across the classes I and II. From Table I we see that on average, SIP gives a higher PSNR for class I and SBP gives a higher PSNR for class II. This motivates the definition of class I and II.

Fig. 3, 4 and Table I exemplified that the performance of different reconstruction approaches depends on the type of the image of interest. If the purpose is reconstruction

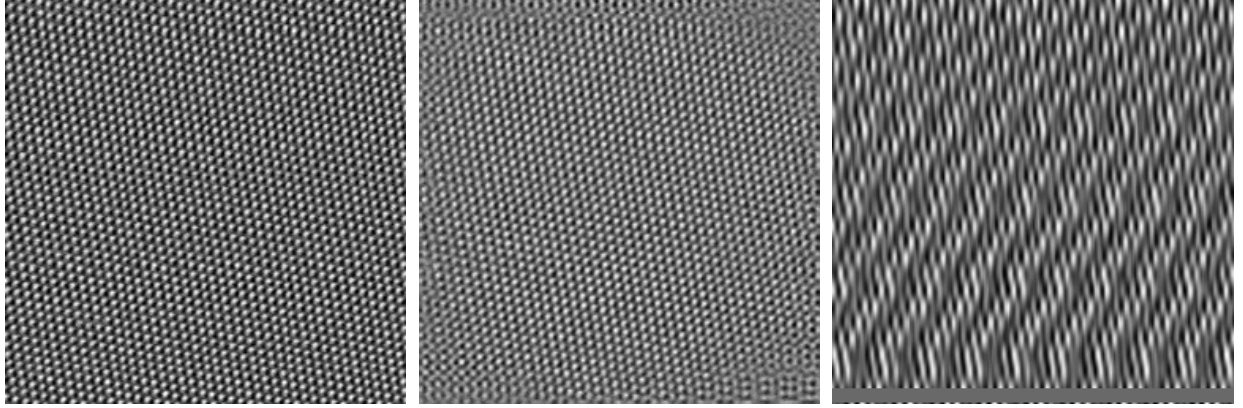
²SPGL1 can use indirect (matrix-free) function evaluation of Az and $A^T y$ using a fast 2D DCT and the masking function h with a complexity of $\mathcal{O}(N \log N + M)$.

³All reconstructions were computed on a standard desktop, Intel Dual Core i5-2410M CPU at 2.3 GHz, 4 GB, with Ubuntu, linux kernel 3.8.0-30-generic and Matlab 7.13.0.564.



(a) Ground truth endothelial cells. (b) SBP, $\kappa = 0.1$, $t = 9.3$ s, PSNR = 20.7 dB. (c) SIP, $\kappa = 0.1$, $t = 0.5$ s, PSNR = 27.6 dB.

Fig. 3: Example comparing spiral sampling and basis pursuit reconstruction (SBP) and subline sampling and interpolation (SIP) for an $(m, n) = (454, 454)$ pixel image of endothelial cells ($\rho_{0.1} = 0.961$).



(a) Ground truth atomic lattice. (b) SBP, $\kappa = 0.1$, $t = 1.8$ s, PSNR = 20.2 dB. (c) SIP, $\kappa = 0.1$, $t = 0.2$ s, PSNR = 14.0 dB.

Fig. 4: Example comparing spiral sampling and basis pursuit reconstruction (SBP) and subline sampling and interpolation (SIP) for an $(m, n) = (256, 254)$ pixel image of an atomic lattice ($\rho_{0.1} = 0.001$).

Average PSNR [dB]	$\kappa = \tau = 0.05$	$\kappa = \tau = 0.10$
Class I, $\mathcal{I}(\tau)$	18.4 / 17.4	20.2 / 18.2
Class II, $\mathcal{J}(\tau)$	15.5 / 16.7	16.6 / 18.7

Table I: Average reconstruction quality in PSNR in dB for different sampling ratios κ according to each class of images. The data are given as SIP / SBP. $|\mathcal{I}(0.05)| = 21$, $|\mathcal{J}(0.05)| = 11$ and $|\mathcal{I}(0.1)| = 28$, $|\mathcal{J}(0.1)| = 4$.

of class I type images, then SIP is preferable. If the purpose is reconstruction of class II type images, then SBP based reconstruction is preferable. As also argued previously, interpolation cannot reconstruct aliased high-frequency information. On the other hand, basis-pursuit can reconstruct all frequencies, including aliased high-frequencies (provided that the image is sufficiently compressible).

V-B. Sequential acquisition

In a standard setup where we first acquire the data and then reconstruct, the user/operator must wait until a complete data acquisition and reconstruction is completed. A related approach is to take a batch of samples, then compute a reconstruction while the AFM equipment acquires a new batch of samples. The user thus monitors the preview image as the image quality increases from each batch of samples to the next and can decide whether the image region is of interest or not. The approach in Sec. V-A can then be seen as a one-batch approach.

Fig. 5 shows the reconstructed images for one- and five-batch samples. Each batch is obtained as a spiral sampling pattern with $\kappa = 0.02$ similar to Fig. 1 but the spiral

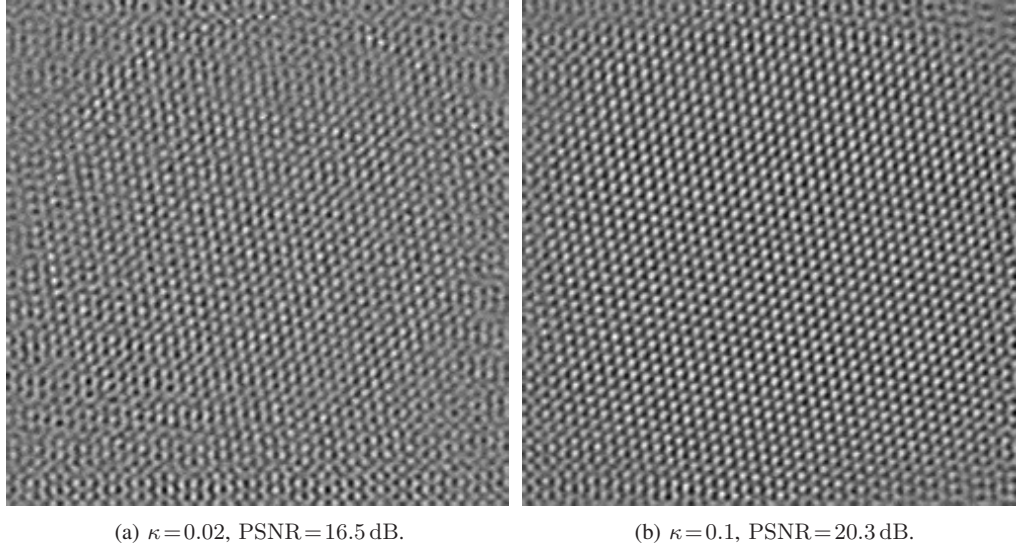


Fig. 5: Two stages sequential acquisition using a spiral sampling pattern. Ground truth is given in Fig. 4(a).

for each batch has different phase. For Fig. 5(a) we have $\kappa = 0.02$ and for Fig. 5(b): $\kappa = 5 \cdot 0.02 = 0.1$. As expected, the image quality increases as κ increases. We see that the visual quality and PSNR of sampling $\kappa = 0.1$ in one batch Fig. 4(b) five batches Fig. 5(b) are very similar. Sequential reconstruction hence has the ability to initially present low quality and then increase quality as more samples are acquired, which is suitable for previewing and operating the AFM equipment.

VI. CONCLUSION AND DISCUSSION

This paper focused on and analyzed the AFM under-sampling problem. The problem can be interpreted as an interpolating or inpainting problem to which there exist many approaches [15], [11]. Of the methods suggested in the literature [9], [4], [8] for the AFM problem, we argued that the preferred approach depends on the frequency content of the image. More complicated methods such as, e.g. dictionary learning may be useful for this application but the method seems too computationally demanding [7]. We focused on noise-less reconstruction. For more noisy images it is expected that interpolation methods are less accurate. On the other hand, basis pursuit has the natural extension basis pursuit denoising for handling noise.

To increase flexibility of the use of AFM it was shown that by changing the phase of the spiral, a new sampling pattern emerges, which provides new measurements that can be exploited in a sequential manner. Specifically, we propose a batch-based acquisition approach with sequential reconstruction which provides even faster imaging preview.

In terms of the sampling pattern, the main disadvantage of the spiral pattern is the lack of sampling in the corners of a square image which caused a certain reconstruction noise

floor. It could have interest to find a middle ground between square and spiral to improve sampling of the corners.

VII. REFERENCES

- [1] P. K. Hansma, G. Schitter, G. E. Fantner, and C. Prater, "High-speed atomic force microscopy," *Science*, vol. 314, pp. 601–602, 2006.
- [2] D. Y. Abramovitch, S. B. Andersson, L. C. Pao, and G. Schitter, "A tutorial on the mechanics, dynamics, and control of atomic force microscopes," in *Proc. American Control Conf. (ACC)*, New York, USA, July 2007, pp. 3488–3502.
- [3] B. Bhushan and O. Marti, *Scanning Probe Microscopy - Principle of Operation, Instrumentation, and Probes*, pp. 573–617, Springer Berlin Heidelberg, 2010.
- [4] S. B. Andersson and L. Y. Pao, "Non-raster sampling in atomic force microscopy: A compressed sensing approach," in *Proc. American Control Conf. (ACC)*, Fairmont Queen Elizabeth, Montreal, Canada, June 2012, pp. 2485–2490.
- [5] G. Schitter and M. J. Rost, "Scanning probe microscopy at video-rate," *Materials Today*, vol. 11, Supplement, pp. 40–48, 2008.
- [6] S. B. Andersson and D. Y. Abramovitch, "A survey of non-raster scan methods with application to atomic force microscopy," in *Proc. American Control Conf. (ACC)*, New York, USA, July 2007, pp. 3516–3521.
- [7] R. B. Farnham, "Processing and inpainting of sparse data as applied to atomic force microscopy imaging," M.S. thesis, Department of Mathematics and Statistics, California State University, Long Beach, California, US, 2012.
- [8] A. Chen, A. L. Bertozzi, P. D. Ashby, P. Getreuer, and Y. Lou, "Enhancement and recovery in atomic force microscopy images," in *Excursions in Harmonic Analysis, Volume 2*, T. D. Andrews, R. Balan, J. J. Benedetto, W. Czaja, and K. A. Okoudjou, Eds., Applied and Numerical Harmonic Analysis, pp. 311–332, Birkhäuser Boston, 2013.
- [9] B. Song, N. Xi, R. Yang, K. W. C. Lai, and C. Qu, "Video rate atomic force microscopy (AFM) imaging using compressive sensing," in *Proc. IEEE Int. Conf. on Nanotech.*, Portland, Oregon, USA, Aug. 2011, pp. 1056–1059.
- [10] I. A. Mahmood, S. O. R. Moheimani, and B. Bhikkaji, "A new scanning method for fast atomic force microscopy," *IEEE Trans. Nanotechnol.*, vol. 10, no. 2, pp. 203–216, 2011.
- [11] M. Elad, *Sparse and Redundant Representations: From Theory to Applications in Signal and Image Processing*, Springer, 2010.

- [12] M. A. Davenport, M. F. Duarte, Y. C. Eldar, and G. Kutyniok, "Introduction to compressed sensing," in *Compressed Sensing: Theory and Applications*. Cambridge University Press, 2012.
- [13] Y. K. Kong, A. Bazaei, S. O. R. Moheimani, and F. Allgover, "Design and control of a novel non-raster scan pattern for fast scanning probe microscopy," in *Proc. IEEE/ASME Int. Conf. Adv. Intell. Mechatron.*, Kaohsiung, Taiwan, July 2012, pp. 456–461.
- [14] T. Tuma, J. Lygeros, A. Sebastian, and A. Pantazi, "Optimal scan trajectories for high-speed scanning probe microscopy," in *Proc. American Control Conf. (ACC)*, Fairmont Queen Elizabeth, Montreal, Canada, June 2012, pp. 3791–3796.
- [15] T. F. Chan and J. Shen, *Image Processing and Analysis: Variational, PDE, Wavelet, and Stochastic Methods*. SIAM, Philadelphia, 2005.
- [16] A. Maleki and D. L. Donoho, "Optimally tuned iterative reconstruction algorithms for compressed sensing," *IEEE J. Sel. Top. Sign. Process.*, vol. 4, no. 2, pp. 330–341, Apr. 2010.
- [17] E. van den Berg and M. P. Friedlander, "Probing the Pareto frontier for basis pursuit solutions," *SIAM J. Sci. Comput.*, vol. 31, no. 2, pp. 890–912, 2008.